water

MDPI

Article

Carbon Dioxide Emissions from the Littoral Zone of a Chinese Reservoir

Meng Yang [1,2], John Grace [3], Xuemeng Geng [2,4], Lei Guan [2,5], Yamian Zhang [2], Jialin Lei [2], Cai Lu [2] and Guangchun Lei [2,*]

1 Key Laboratory of Ecosystem Network Observation and Modeling, Institute of Geographic Sciences and Natural Resources Research, Chinese Academy of Sciences, Beijing 100101, China; yangmeng@igsnrr.ac.cn
2 School of Nature Conservation, Beijing Forestry University, Beijing 100083, China; xuemeng17@foxmail.com (X.G.); gl4211@163.com (L.G.); yamian183@163.com (Y.Z.); leijialinbjfu@foxmail.com (J.L.); lucai.wetland@foxmail.com (C.L.)
3 School of Geosciences, The University of Edinburgh, Edinburgh EH9 3FF, UK; jgrace@ed.ac.uk
4 Beijing Shoufa Tianren Ecological Landscape Co., Ltd., Beijing 102600, China
5 School of Humanities and Laws, Tianjin Polytechnic University, Tianjin 300387, China
* Correspondence: guangchun.lei@foxmail.com; Tel.: +86-10-6233-6717

Received: 3 May 2017; Accepted: 14 July 2017; Published: 19 July 2017

Abstract: The continuous increase in the number of reservoirs globally has raised important questions about the environmental impact of their greenhouse gases emissions. In particular, the littoral zone may be a hotspot for production of greenhouse gases. We investigated the spatiotemporal variation of CO_2 flux at the littoral zone of a Chinese reservoir along a wet-to-dry transect from permanently flooded land, seasonally flooded land to non-flooded dry land, using the static dark chamber technique. The mean total CO_2 emission was 346 mg m^{-2} h^{-1} and the rate varied significantly by water levels, months and time of day. The spatiotemporal variation of flux was highly correlated with biomass, temperature and water level. Flooding could play a positive role in carbon balance if water recession occurs at the time when carbon gains associated with plant growth overcomes the carbon loss of ecosystem. The overall carbon balance was analysed using cumulative greenhouse gases fluxes and biomass, bringing the data of the present study alongside previously published, simultaneously measured CH_4 and N_2O fluxes. For the growing season, 12.8 g C m^{-2} was absorbed by the littoral zone. Taking CH_4 and N_2O into the calculation showed that permanently flooded sites were a source of greenhouse gases, rather than a sink. Our study emphasises how water level fluctuation influenced CO_2, CH_4 and N_2O in different ways, which greatly affected the spatiotemporal variation and emission rate of greenhouse gases from the littoral zone.

Keywords: greenhouse gas fluxes; reservoir; littoral zone; flooding

1. Introduction

Greenhouse gas (GHG) emissions from reservoirs have attracted much attention, not only because of the substantial contribution they already make to global GHG budgets but also because large reservoirs are still being created in many parts of the world, especially Southeast Asia, South America and Africa [1,2]. When reservoirs are designed for power generation they are often assumed to be 'clean' when the alternative to hydropower involves combustion of fossil fuels or the use of nuclear power stations. Yet even this assumption has been questioned [3–6], and, in the absence of data on the emissions of CH_4, N_2O and CO_2, there are few cases where the full environmental costs and benefits have been investigated.

Years ago, working with limited data, the global CO_2 emissions from reservoirs were estimated to be 273 Tg C $year^{-1}$, which was then equivalent to 4% of other anthropogenic emissions [3].

However, the latest global estimate was much lower when including more data and environments. Deemer et al. [4] reports 36.8 Tg C year^{-1} while the number from Li & Zhang [5] reported here is 82 Tg C year^{-1}. Those researchers also emphasized the importance of drawdown and downstream emissions which can represent up to 42% of total emissions, as well the large degree of uncertainty caused by spatial and temporal variation [4–7]. Indeed, much uncertainty remains. For example, one recent study in CO_2 concentrations and fluxes of five tropical reservoirs pointed out that ignoring the spatial variability can lead to more than 25% error in the total system flux [8]. CO_2 emission are likely to be underestimated by approximately 40% when ignoring the diel emission difference and frequent synoptic weather events which may induce CO_2 emission pulses at longer time scales [7].

Of particular interest is the intensive and highly varied greenhouse gas emission around the margins of reservoirs. As a characteristic of the littoral zone, flooding influences a plethora of environmental variables, which include vegetation change/succession, hydrostatic pressure, soil aeration, nutrients, and soil/sediment temperatures, all of which add to the variation in the greenhouse gas production and emission rate [9–14]. During the flooding phase, higher variability of CO_2 emission was observed within the various sections of each temporary zone (i.e., inundated, emerged-unvegetated and emerged-vegetated) than among the zones [12]. Exposure of sediment could activate oxidase and hydrolase (two magnitudes higher), leading to more greenhouse gases emission [15]. When the water table decreased from 5 cm aboveground to 5 cm belowground, the total soil respiration of the growing season increased from 720 g m^{-2} to 1490 g m^{-2} [16]. Although the influences of water level fluctuation on greenhouse gases emission have been observed, the paucity of studies on these various effects constrain the overall understanding on greenhouse gases emission from drawdown areas.

Elsewhere, we have reported the emissions of CH_4 and N_2O from the Miyun Reservoir, and we demonstrated that this littoral zone can be regarded as a hot spot for emissions [17,18]. In the present paper, we evaluate (i) the spatiotemporal variation of CO_2 emissions from the littoral zone; and (ii) the influence of environmental factors, especially flooding. Finally, we conclude our analysis by considering the complete greenhouse gas balance of the littoral zone in which the contributions of CH_4 and N_2O are considered alongside CO_2.

2. Materials and Methods

2.1. Study Area and Sampling Sites

The research was carried out at the littoral zone of the Miyun Reservoir (40°29′ N, 116°50′ E), Beijing, China. Its catchment is classified as warm temperate semi-humid monsoonal climate, having a hot summer and a cold winter. The growing season is from April to November. Precipitation is unequally distributed across the typical year (80% in summer) [19]. The annual water level difference is around 1 to 5 m [20].

Along the transect from water to upland, the sampling sites are grouped at 5 different heights (Figure 1), i.e., (1) DW: deep water area; (2) SW: shallow water area; (3) SF: seasonally flooded area; (4) SFC: 'control area' for the seasonally flooded area, which had similar vegetation and soil moisture as site SF before SF was flooded, but escaped the flood in August and September because of its 1-m-higher elevation; (5) NF: non-flooded area, which usually floods once per several years but was not flooded in the sampling year. Three plots supporting somewhat different vegetation types were selected within each height band, for the species details see Supplementary Materials Table S1. There were 15 plots in total, four replicates in each plot.

The study area and the experimental design of the present research was exactly the same as in the previous CH_4 and N_2O study [17,18].

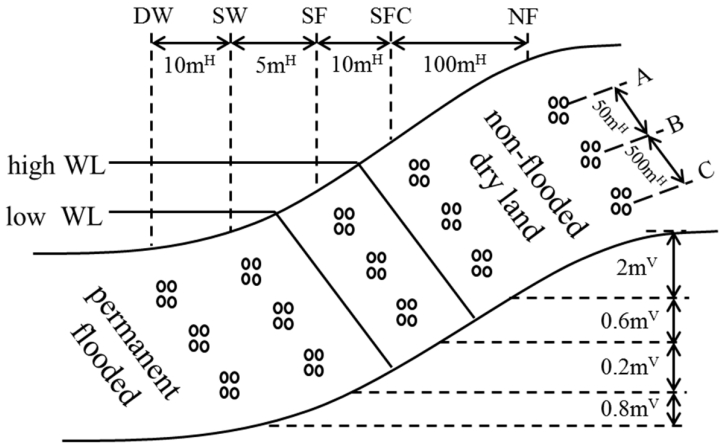

Figure 1. Experimental design [17,18]. WL: water level. The difference between high WL and low WL was caused by summer flooding. m^H indicates meters in horizontal; m^V indicates meters in vertical. The sites are grouped at different heights. DW: deep water site; SW: shallow water site; SF: seasonally flooded site; SFC: 'control site' for the seasonally flooded site; NF: non-flooded site. A, B and C denote samples from different vegetation types within each height band. For more details on water depth and other environmental parameters, see Table 1, Figures 2 and S1.

Table 1. Physicochemical properties (Mean ± SE (standard error)) of soil/sediment of each site. DW: deep water site; SW: shallow water site; SF: seasonally flooded site; SFC: 'control site' for the seasonally flooded site; NF: non-flooded site. A, B and C denote samples from different vegetation types within each height band, species details see Table S1.

Site	Bulk Density (g cm^{-3})	pH	Total Carbon (g kg^{-1})	Total Nitrogen (g kg^{-1})	NH_4^+ (mg kg^{-1})	NO_3^- (mg kg^{-1})
DW-A	1.03 ± 0.03	7.95 ± 0.01	19.81 ± 0.77	1.57 ± 0.06	22.98 ± 1.16	8.1 ± 1.24
DW-B	1.03 ± 0.03	7.95 ± 0.01	19.81 ± 0.77	1.57 ± 0.06	23 ± 0	8.1 ± 0
DW-C	1.03 ± 0.03	7.84 ± 0.08	22.63 ± 0.48	1.8 ± 0.03	22.93 ± 0.64	5.95 ± 0.3
SW-A	1.38 ± 0.03	8.03 ± 0.04	8.2 ± 0.65	0.65 ± 0.04	24.36 ± 0.44	6.89 ± 0.56
SW-B	1.38 ± 0.02	8.13 ± 0.1	9.19 ± 0.29	0.66 ± 0.02	25.72 ± 0.62	7.55 ± 0.37
SW-C	1.4 ± 0.05	8.09 ± 0.06	9.81 ± 1.45	0.81 ± 0.13	32.79 ± 6.22	5.94 ± 0.74
SF-A	1.39 ± 0.04	8.13 ± 0.06	7.23 ± 0.27	0.56 ± 0.02	24.67 ± 3.73	6.13 ± 0.48
SF-B	1.43 ± 0.02	7.98 ± 0.03	8.22 ± 0.64	0.67 ± 0.04	28.44 ± 2.42	6.59 ± 1.01
SF-C	1.43 ± 0.05	8.03 ± 0.02	7.13 ± 0.55	0.64 ± 0.03	30.01 ± 3.75	6.6 ± 0.92
SFC-A	1.5 ± 0.04	8.61 ± 0.02	8.2 ± 0.23	0.72 ± 0.01	4.13 ± 0.23	7.86 ± 0.41
SFC-B	1.49 ± 0.02	8.48 ± 0.06	8.13 ± 0.44	0.71 ± 0.04	4.23 ± 0.39	7.61 ± 0.19
SFC-C	1.4 ± 0.04	7.76 ± 0.03	3.45 ± 0.15	0.36 ± 0.01	3.08 ± 0.09	7.54 ± 0.38
NF-A	1.66 ± 0.08	8.27 ± 0.08	2.19 ± 0.62	0.14 ± 0.06	19.22 ± 0.76	5.76 ± 1.71
NF-B	1.62 ± 0.02	7.59 ± 0.06	5.5 ± 0.3	0.47 ± 0.02	24.16 ± 1.17	4.39 ± 0.32
NF-C	1.45 ± 0.01	8.15 ± 0.05	6.22 ± 0.18	0.57 ± 0.02	27.07 ± 1.29	12.81 ± 0.66

2.2. CO_2 Flux and Environmental Factors Measurements

CO_2 flux was observed using the dark chamber and gas chromatography techniques (for details see [17,18]). The gas samples were repeatedly taken six times in the year to cover the different seasons (November 2011, May, July, August, September and October 2012) and covering the transition in and out of the flooding season. Also to capture diurnal variation, the plots were repeatedly sampled seven times per day (local time: 6, 9, 12, 15, 18, 21 and 24 h). To determine the effect of aboveground vegetation on flux, one more flux measurement was taken at 9 a.m. the following day (after seven times sampling for diurnal variation), with the aboveground plant material removed. Chambers were reset into new positions near the old positions each sampling month. For more details on the water depth and other environmental parameters, see Figure S1 and Table 1.

In order to calculate the cumulative carbon balance, the belowground biomass of every replicate in the chamber of SW, SF and NF was weighed after rinsing and drying at 80 °C to constant mass. The belowground biomass of DW was not determined directly because of manipulation difficulty. To protect the sampling area from serious interference, root biomass was collected just one time in November 2011. The observed average root/shoot ratio of 0.41 was used for each area in the total biomass calculation. The aboveground biomass of every replicate in the chamber was weighed every campaign after drying at 80 °C to constant mass.

The air temperature was observed at the start and end of each gas sampling at every plot by means of a digital thermometer (JM624, Jinming, Henan, China). The standing water depth was measured using a metre stick after gas sampling at DW, SW and SF (during flooding). The water level of SF (before and after flooding) and SFC was shallow. Therefore, a 1-m high PVC (Polyvinyl chloride) tube with small side holes was inserted vertically into the soil under the chamber after all monthly gas sampling was complete, allowing two h for the water level to equilibrate before measuring the level. The water level of site NF was calculated according to the elevation measured by a Global Navigation Satellite System receiver (BLH-L90, Daheng International, Hong Kong, China).

Soil samples at site DW, SW, SF and NF were collected manually (0–30 cm) at each replicate location in November 2011, except site SFC in October 2012. Soil NH_4^+, NO_3^-, pH, total carbon, total nitrogen and bulk density were then analysed. Weekly precipitation, daily air temperature and daily water level were accessed online. Wind speed, soil water content and dissolved oxygen in water were recorded in situ, for detailed methods, see Yang et al. [17].

2.3. Greenhouse Gases Balance Assessment

To calculate the cumulative greenhouse gas emissions, models were needed for day-to-day flux simulation. Emission models were selected using the AIC (Akaike information criterion) criterium according to Burnham et al. [21]. Following a paper which represents a method for NEE (net ecosystem exchange) assessment based on chamber technique, we choose soil apparent respiration (SAR, sum of root respiration and heterotrophic respiration) for evaluating the carbon balance. After model selection, daily SAR, CH_4 and N_2O emissions were simulated and then used for C balance calculations, combined with daily biomass changes following [22] with Equation (1):

$$\text{Balance} = (F_{SAR} \times \alpha + F_{CH4} \times GWP_{100} + F_{N2O} \times GWP_{100}) \times \frac{12}{44} - Biom \times \beta \quad (1)$$

where F_{SAR} is the soil apparent respiraton. α is the ratio of heterotrophic respiration to soil apparent respiration, assuming a value of 0.55 [22,23]. GWP_{100} is Global Warming Potential over 100-year time-span, which was taken as 34 and 298 for CH_4 and N_2O respectively [24]. *Biom* is the total biomass including both shoot and root. β is the carbon content of biomass, which was taken as 40% [25].

In the simulations, the total biomass growth was represented as a linear interpolation of the biomass data. Daily water depth was calculated using the daily water level and elevation of each area. Soil properties were assumed stable during the simulated season.

2.4. Statistical Analysis

Flux differences among the water levels, months and times of day were tested using a three-way ANOVA, and then using LSD (Least Significant Difference) for multiple comparisons. All the analyses above were performed using IBM SPSS Statistics (version 19.0, IBM, New York, NY, USA).

3. Results

3.1. CO_2 Flux and Environmental Influences

The fluxes (total respiration) were significantly different among water levels, months and times of day (Figure 2 and Table 2). The mean CO_2 flux from the littoral zone was 346 mg m^{-2} h^{-1}, ranging

from −98 to 2274 mg m^{-2} h^{-1}. Negative flux was rarely observed (sometimes at DW-A and DW-B, 8 times in all 324 observations).

Spatially, the flux increased along the gradient from the deep water (114 ± 10 mg m^{-2} h^{-1}) to the non-flooded area (723 ± 10 mg m^{-2} h^{-1}), Figure 2. The efflux from the seasonal flooded area (229 ± 10 mg m^{-2} h^{-1}) was much lower than its control area (629 ± 14 mg m^{-2} h^{-1}), Figure 2. Biomass and water level showed a good correlation with variation of the CO_2 flux among water levels, the r^2 of the linear regression being 0.99 and 0.80 respectively.

Temporally, clear monthly and diurnal variations were observed, Figure 2. The flux peaked in August and mid-day respectively. Temperature showed the best correlation with the temporal variation of CO_2 flux. The change patterns of monthly average water level and CO_2 emission of all sites were similar, but linear regressions were not significant ($p = 0.06$). The variable 'Biomass' could not explain monthly CO_2 variation, the r^2 of linear regression being as low as 0.003 ($p = 0.92$).

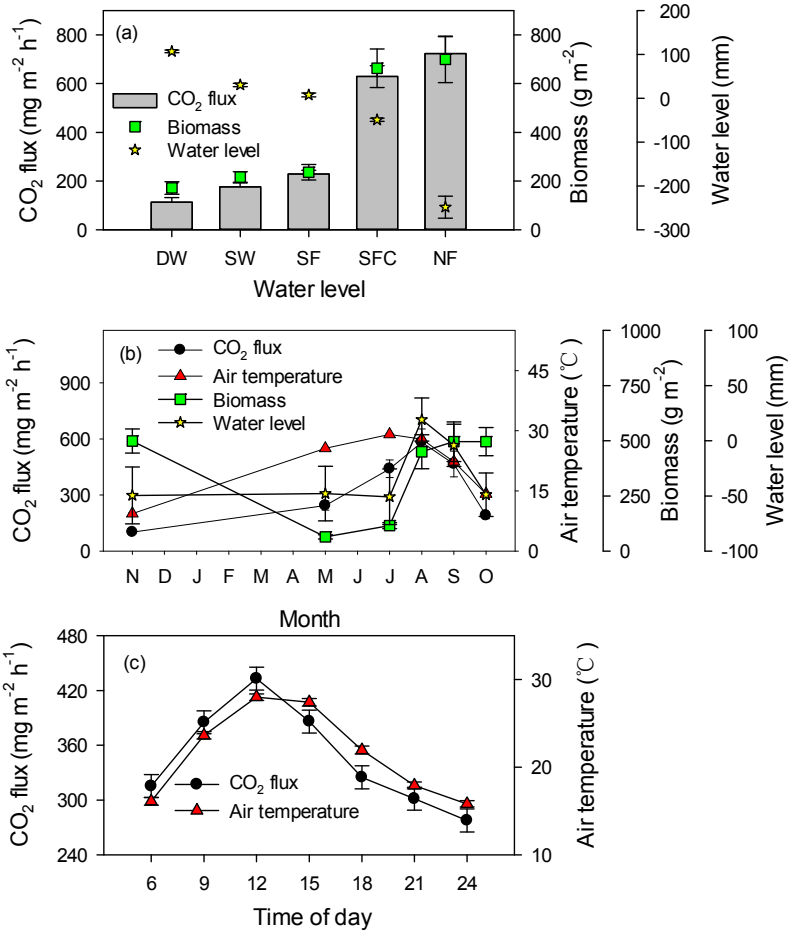

Figure 2. Spatiotemporal variation of CO_2 flux and environments (mean ± SE). (**a**) CO_2 flux, biomass and water level of each area. Linear regressions: $Flux_{CO2} = 1.07 \times Biomass - 51.7$, $n = 5$, $p < 0.01$, $r^2 = 0.99$; $Flux_{CO2} = -0.43 \times$ Water level + 129.2, $n = 5$, $p = 0.04$, $r^2 = 0.80$. (**b**) CO_2 flux, temperature, biomass and water level of each month. Linear regressions: $Flux_{CO2} = 19.43 \times$ Temperature − 80.9, $n = 6$, $p = 0.05$, $r^2 = 0.66$; $Flux_{CO2} = 484.9 \times$ Water level + 4.9, $n = 6$, $p = 0.06$, $r^2 = 0.63$; regression with biomass was not significant, $p = 0.92$. (**c**) CO_2 flux and temperature of each time of day. Linear regression: $Flux_{CO2} = 10.18 \times$ Temperature + 126.8, $n = 7$, $p < 0.01$, $r^2 = 0.86$. DW: deep water site; SW: shallow water site; SF: seasonally flooded site; SFC: 'control site' for the seasonally flooded site; NF: non-flooded site. Some error bars are invisible because they are too small to see.

To determine the effect of biomass on fluxes and provide data for the assessment of gas balance, fluxes after removal of aboveground plants were measured. Compared to the fluxes with the shoots intact, the differences between sites largely vanished in term of CO_2 emission among the plots in the same water condition (Figure 3). Removal of the aboveground parts demonstrated that the contribution of aboveground vegetation to total respiration was 27–75%, averaged at 52%.

Using the AIC criterium, seven variables went into the best CO_2 model, i.e., shoot biomass, air temperature, water depth, soil pH, soil NH_4^+, soil total carbon and soil total nitrogen.

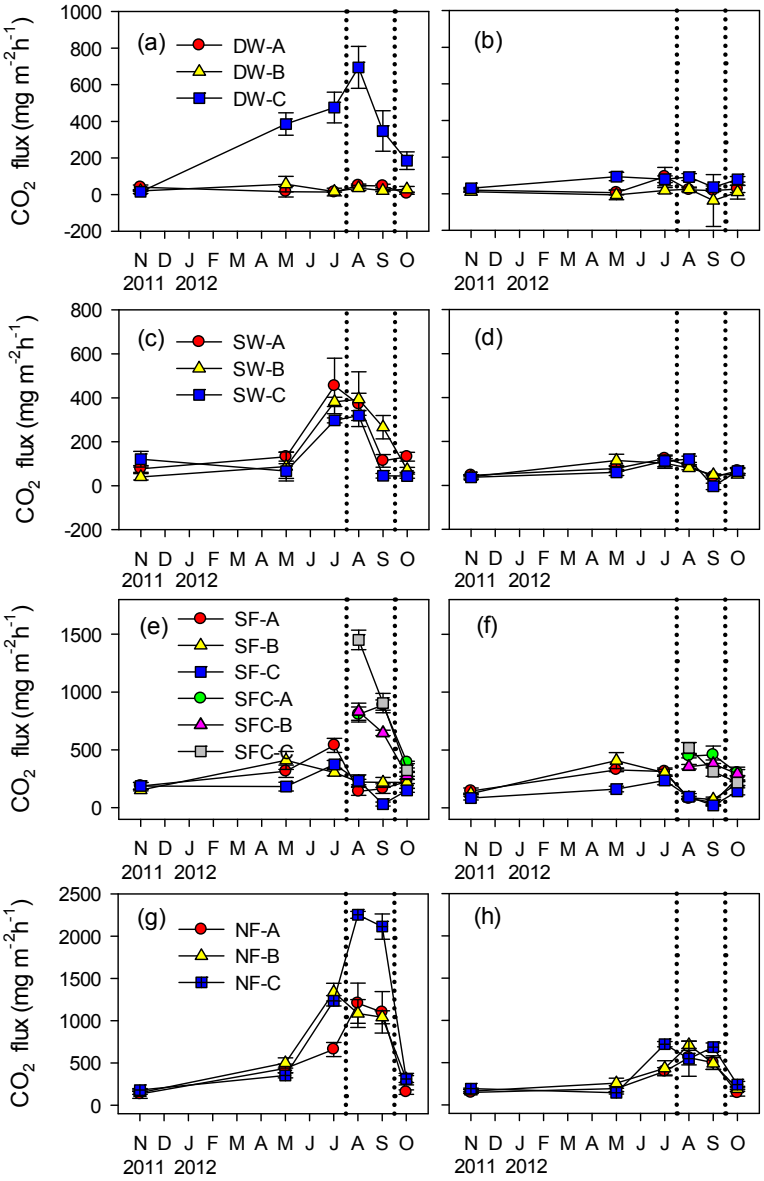

Figure 3. Influence of aboveground plant on monthly and spatial variation of CO_2 flux (mean ± SE). Subfigures show the CO_2 flux of site DW (**a**,**b**), SW (**c**,**d**), SF and its 'control site' SFC (**e**,**f**), and NF (**g**,**h**) respectively, with and without aboveground plant. The left plots were flux with aboveground vegetation while the right plots were flux after aboveground vegetation being removed. Days between dashed vertical lines were flooding period when seasonal flooded area was under water.

Table 2. ANOVA table to test the effects of water level, sampling month and time of day on CO_2 flux.

Effect	Degrees of Freedom	*F*-Value	*p*-Value
Water level	4	644.6	<0.001
Month	5	226.3	<0.001
Time of day	6	19.2	<0.001
Water level × Month	17	97.4	<0.001
Water level × Time of day	24	4.1	<0.001
Month × Time of day	30	1.8	0.004
Water level × Month × Time of day	102	1.1	0.225
Error	2068		

3.2. Greenhouse Gas Balance

For daily greenhouse gas fluxes, several simulation models we examined using the AIC criterium (Table 3). Of all three gases, CO_2 (soil apparent respiration) is the one that showed the strongest correlation with environmental variables (r^2 = 0.54). The correlation between N_2O emission and environmental variables was weak (r^2 = 0.15).

Table 3. Model selection for the daily flux simulation. Only the best three models were shown. F: flux (mg m^{-2} h^{-1}); B: shoot biomass (g m^{-2}); T: air temperature (°C); WD: water depth (cm); PH: soil pH; NH: soil NH_4^+ (mg kg^{-1}); TC: soil total carbon (g kg^{-1}); BD: soil bulk density (g cm^{-3}); NO: soil NO_3^- (mg kg^{-1}); SAR: root and soil respiration. Sampling size was 324. AIC: Akaike information criterion.

Gases		Model	SS	K	AIC Value
CO_2 (SAR)	1	F = −1352.65 + 0.11B + 9.05T − 0.52WD + 174.03PH − 3.24NH − 32.97TC + 364.52TN	5.7×10^7	8	1390.8
	2	F = −1459.12 + 0.12B + 9.21T − 0.55WD + 186.69PH − 3.25NH − 3.76TC	5.8×10^7	7	1391.2
	3	F = −1872.2 + 0.12B + 9.49T − 0.64WD + 231.36PH − 3.04NH	5.9×10^7	6	1391.4
CH_4	1	F = 19.580 + 3.255TN + 0.091T + 0.009WD − 4.121PH + 7.833BD	1942	6	264.0
	2	F = 18.641 + 0.256TC + 0.091T + 0.008WD − 3.960PH + 7.611BD	1945	6	264.2
	3	F = 17.992 + 3.068TN + 0.091T + 0.008WD − 3.663PH + 6.956BD − 0.105NO	1926	7	264.8
N_2O	1	F = 0.001 × (−37.096 + 3.458NO + 0.551T − 0.019WD + 0.302NH)	1.5×10^5	5	875.774
	2	F = 0.001 × (−29.243 + 3.350NO + 0.547T − 0.018WD)	1.5×10^5	4	875.776
	3	F = 0.001 × (−26.057 + 3.129NO + 0.495T)	1.6×10^5	3	876.087

The greenhouse gas balance is presented as cumulative carbon fluxes and balances (Figure 4). Including CH_4 and N_2O into the consideration of GHG-balance brought noticeable changes in the overall balances, especially for site DW and SW, turning the littoral area from a sink to a source of greenhouse gases. In deep water, the growth of biomass was insufficient to absorb more than a tiny fraction of the observed emissions (Figure 4a). In shallow water conditions (SW) fixation of carbon as biomass offset a substantial part of the emissions, but there was however a net loss of greenhouse gases from the sites (Figure 4b). For the growing season (184 days), the budget of permanent flooded areas DW and SW, in terms of C-equivalent, was 123.3 g C m^{-2} and 5.1 g C m^{-2}. In the seasonal flooded area, regrowth of vegetation after water recession accumulated 227 g m^{-2} in term of new biomass from exposure of the land at the end of October. The increasing in biomass converts SF from being a greenhouse gas source to a sink (the balance changed from 33 to −70 g C m^{-2}, Figure 4c). In the non-flooded area, the carbon absorbed by the growing vegetation was substantial (note the change of scale of the y-axis) allowing it to be the largest sink of 109.1 g C m^{-2}, although it also had the largest emission of 225.0 g C m^{-2}. For the growing season, 12.8 g C m^{-2} was absorbed on average.

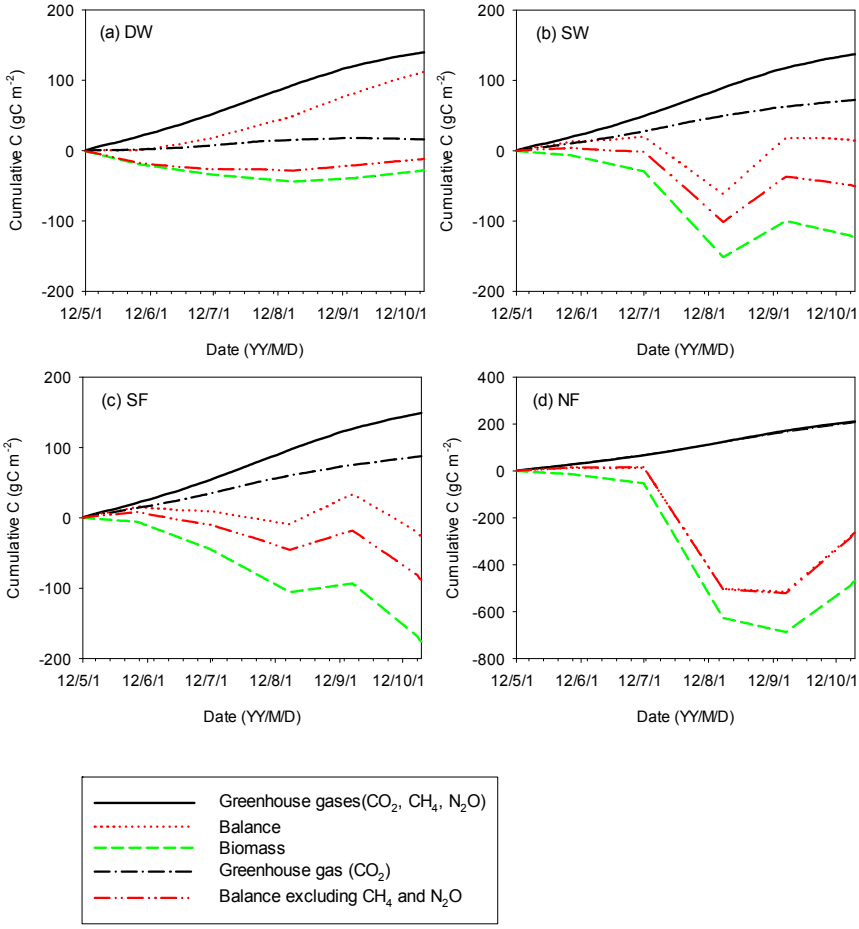

Figure 4. Cumulative greenhouse gas fluxes, biomass and the balance of the growing season. Subfigures show the cumulative greenhouse gas fluxes, biomass and the balance of site DW (**a**), SW (**b**), SF (**c**) and NF (**d**) respectively. Fluxes of CH_4 and N_2O were converted by multiplying by Global Warming Potential. Balance was the difference in terms of C-equivalent between greenhouse gases emission and biomass. Balance excludes CH_4 and N_2O was the difference in terms of C-equivalent between CO_2 emission and biomass. Positive values indicate C loss while negative values indicate C gain.

4. Discussion

4.1. CO_2 Flux

The margins of reservoirs and lakes are often overlooked as potential sources and sinks of greenhouse gases. Most researchers have focused on the water body itself (see [26–28], disregarding the green zone at the water's edge. For lakes especially, and for reservoirs to a lesser extent, there are many investigations of the CO_2 flux from the open water surface, sometimes measured directly using chambers or (rarely) obtained from micrometeorological techniques; but more often, fluxes are estimated from a knowledge of the dissolved CO_2 concentration in the water samples [29–32]. Our study helps to redress the balance by providing new observational data from the margins of a reservoir which may be compared to values obtained from open water. In a review of the global literature on lakes, Pace & Prairie (their Table 7.1, [27]) found a range from open water that varied enormously between 21 and 395 mg CO_2 m^{-2} h^{-1} with a mean of 148 mg CO_2 m^{-2} h^{-1}, derived from planktonic and sediment respiration. Recently we have compiled a database of the world literature on reservoirs (supplement Table S3): the mean value of 79 studies at pelagic sites was 103 mg CO_2 m^{-2} h^{-1}. If we take only the Chinese data from the database (n = 10), we have 72 mg CO_2 m^{-2} h^{-1} as the flux from the pelagic zone. In the present (littoral) data set, the total

respiration rates are generally higher, averaging 346 mg CO_2 m^{-2} h^{-1} and of course much higher in the non-flooded area where vegetation flourishes. We conclude that the littoral zone is more active in terms of CO_2 exchange than the open water when compared on a per area basis, and should be taken into account when evaluating the role of water bodies in the carbon cycle, particularly in those reservoirs with a large ratio of littoral: open-water.

4.2. Influences of Environment

The CO_2 emissions differed significantly among the water levels, the months and the different times of day (Figure 2 and Table 2). Biomass and temperature were two important factors determining the spatiotemporal variations [33,34]. For the flux differences among water levels, biomass showed the best fit (r^2 of linear regression was up to 0.99). Comparison between fluxes with and without aboveground vegetation of the 15 sites showed that shoot respiration was responsible for 27–75% of the total CO_2 emission. After removal of the aboveground biomass, the obvious differences among sampling sites under the same water condition vanished (Figure 3). For temporal variation, temperature showed a good fit. The correlations of temperature with fluxes during the different times of day were better than with that of different months. Fluxes of different months were also influenced by other factors, such as the biomass and soil water condition, which could alter the response of respiration to temperature [35]. However, those factors were relatively stable in one day, showing a clearer temperature effect at a daily scale.

Besides biomass and temperature, water condition also influenced the CO_2 exchange. That was reflected in the significant difference between the emissions from flooded sites and non-flooded sites. On the one hand, flooding could inhibit autotrophic respiration by killing flood-intolerant vegetation through lack of oxygen and accumulation of toxic compounds [36,37]. On the other hand, flooding could slow down heterotrophic respiration through limiting aeration [38]. Aerobic respiration results in much more CO_2 production than anaerobic respiration: McNicol and Silver's study showed a 50% decrease of soil respiration caused by limiting aeration [39].

Additionally, change of the water condition could also influence C accumulation as biomass. The seasonally-flooded site was the only area which turned from carbon source to carbon sink in the autumn (Figure 4). The decline was caused by the increased accumulation of biomass. The important role that ephemeral vegetation plays in C fixation has been reported in the marginal area of a river [40]. After water recession, new plants sprouted and grew on the exposed soil. When considering CH_4 flux separately, flooding boosted the emission [18], but when CO_2 exchange was taken into consideration, flooding played a positive role in C gain/loss through addition of biomass (i.e., flooding-induced C gain as biomass was greater than C loss as CH_4 in the present study, Figure 4), which is restricted by flooding time and plant phenology. If water recession occurred in the non-growing season, the process of water level fluctuation would merely increase the CH_4 emission but not the uptake of CO_2. Plants growing in the littoral zone are generally herbaceous. Although extra biomass accumulated after water recession, how much of it can be fixed in the soil after death highly depends on content of recalcitrant compounds, especially lignin, and the weather and hydrology of the following months [41].

4.3. Comparison with Other Greenhouse Gases and the Source/Sink Question

The contribution of CH_4 and N_2O to the balance of greenhouse gases flux was important (CH_4 was most important in the present study, Figure S2), especially for the two permanently flooded sites, i.e., DW and SW. When considering only CO_2, the sites DW and SW were greenhouse gas sinks, absorbing 9.9 g C m^{-2} and 60.9 g C m^{-2}, respectively, in the growing season. When CH_4 and N_2O are included in the calculation, DW and SW are revealed as greenhouse gas sources, losing the equivalent of 123.3 g C m^{-2} and 5.1 g C m^{-2}, respectively. The importance of CH_4 and N_2O emission in greenhouse gas balances have been reported in numerous previous studies, for example coppice, grassland and cropland [42–44]. A simulation study on the greenhouse gases balance of North American terrestrial ecosystems showed that emissions of CH_4 and N_2O from wetland overturned the

climate cooling effect induced by the CO_2 sink (2.2 times) and offset, by 0.3, 0.75 and 0.52 times, the sink effect of the forest, grassland and cropland respectively [45]. Our study agrees with the ideas that all three gases should be accounted in global change research and non-CO_2 emissions could well be the dominant contributors in some wetland ecosystems.

For the growing season, the CO_2, CH_4 and N_2O exchange of the four different environments DW, SW, SF and NF was 123.3, 5.1, −70.0 and −109.1 g C m^{-2}, respectively (positive value indicates loss, negative value indicates gain). Our observed balances were more or less different from results of the previous studies. For example, the budget of a Danish riparian wetland was −450 to 40 g C m^{-2} (over 8 months) [46]. A bog undergoing restoration in Canada absorbed 6 ± 28 g C m^{-2} $year^{-1}$ [47]. A peatland in Estonia lost 103 to148 g C m^{-2} $year^{-1}$ [48]. The comparison with the three temperate wetlands indicated that our estimation was within a reasonable range, although three reference ratios were taken to obtain the balance calculation, i.e., root to shoot ratio, carbon content of biomass and the ratio of heterotrophic respiration to soil apparent respiration.

Usage of an estimated reference values introduces uncertainties to varying degrees. The belowground biomass of 9 sites (4 replicates for each site, the 3 sites of DW were abandoned because of practical manipulation difficulties) was investigated in November 2011. To decrease disturbance to the sampling area, root biomass was measured only once. Root to shoot ratio ranged from 0.13 to 0.93, and the average was 0.41. Ratios of root to shoot are expected to change spatially and temporally along environment gradients, even for a given species, such as the soil water content and the available organic matter. The calculation of the C balance is sensitive to this ratio: if we take the extremes (0.13 and 0.93), the balance becomes 22.9 g C m^{-2} and −79.0 g C m^{-2}.

The carbon content of vegetation is relatively constant across a wide variety of species. Reference ratios are sometimes provided to enable simple carbon cycle calculations. The IPCC (Intergovernmental Panel on Climate Change) recommends 0.5 for wood and 0.4 for herbs [25]. The FAO (Food and Agriculture Organization of the United Nations) recommend 0.475 for wood [49]. In the present study, we assumed 0.4 as the vegetation is predominantly herbaceous. A study of the carbon content of 15 wetland plants of which 8 species are in the same family as the plants growing in our sampling area gives an impression of the likely variation: the carbon content was from 0.35 to 0.54 [50]. If we replaced 0.4 by 0.35 and 0.54, the estimated average balance will be 9.7 and −75.6 g C m^{-2}.

Following a study on methods of NEE evaluation based on the chamber technique [22], the ratio of heterotrophic respiration to soil apparent respiration in the present research was assumed to be 0.55. In reality, this ratio may be expected to vary across time and space. Tang et al. reported a ratio of 0.56 during the growing season and 0.16 during the non-growing season with an annual average of 0.44 [51]. Hanson et al. summarised 50 studies working with these ratios and found a wide range from below 0.1 to above 0.9 [52]. If, *in extremis*, we were to take 0.1 and 0.9 for the present assessment, the balance would be −96.0 g C m^{-2} and 52.0 g C m^{-2}. There may be other sources of error, for example the linear models (Table 3) used in evaluating the balance were themselves rather weak, especially the N_2O model. However, the N_2O emission (6.8 μg m^{-2} h^{-1} on average, see [17]) was small compared to that of CO_2 and CH_4 (1.3 mg m^{-2} h^{-1} on average, see [18]), and so we would not expect any big influence on the overall balance from the lack-of-fit of the N_2O model. Finally, for the flooded areas, the flux observed after removal of shoots might include respiration of the phytoplankton. This fraction would have introduced uncertainties in the budget assessment since the ratio of heterotrophic respiration to soil apparent respiration was from work on non-flooded soil.

Notwithstanding the caveats mentioned above, our study in the littoral zone of the Miyun Reservoir supports the view that the margins of lakes may be hotspots of greenhouse gases emission. The study emphasizes how water level fluctuation may play an important role in influencing the emissions, e.g. increasing CH_4 emission through O_2 consumption by decomposing of plant tissue during flooding [18], increasing N_2O emission by providing suitable moisture content during water recession [17,53], and decreasing CO_2 emission by regrowth of vegetation after water recession (this study).

Supplementary Materials: The following are available online at http://www.mdpi.com/2073-4441/9/7/539, Figure S1: Environmental characteristics (Mean ± SE) of each sampling area; Figure S2: Simulated flux of each area of the sampling growing season; Table S1: Dominant plant species at each plot in different months; Table S2: Spearman's Rank Correlation (*r*) between flux and environmental variables.; Table S3: CO2 flux from open water areas of reservoirs around the world.

Acknowledgments: This study was financially supported by: (1) Special Foundation for Basic Scientific and Technological Research Program under grant 2013FY111800; (2) State Forestry Administration of China under grant 200804005; (3) Institute of Geographic Sciences and Natural Resources Research under grant Y6V60220YZ; (4) CAS China Scholarship Council. We thank Yifei Jia, Yi Zhu, Yunzhu Liu, Shengwu Jiao, Linlu Shi, Rui Li, Duoduo Feng, Hairui Duo, Lei Jing, Qing Zeng, Chu Lang, Xu Luo, Jiayuan Li, Yonghong Gao, Defeng Bai, Siyu Zhu, and Jianing Xu for their great support during the course of this study. We also thank Beijing North Miyun Reservoir Eco-agriculture Co. Ltd. for granting us permission to conduct the study on its land. We sincerely appreciate the anonymous reviewers who provide valuable suggestions and kind help on this paper.

Author Contributions: G.L., M.Y. and C.L. conceived and designed the experiments; M.Y., X.G., C.L., L.G., Y.Z. and J.L. performed the experiments; M.Y. and J.G. analyzed the data; M.Y. and J.G. wrote the paper.

Conflicts of Interest: The authors declare no conflict of interest. The founding sponsors had no role in the design of the study; in the collection, analyses, or interpretation of data; in the writing of the manuscript, and in the decision to publish the results.

References

1. Yang, L.; Lu, F.; Zhou, X.; Wang, X.; Duan, X.; Sun, B. Progress in the studies on the greenhouse gas emissions from reservoirs. *Acta Ecol. Sin.* **2014**, *34*, 204–212. [CrossRef]
2. Zarfl, C.; Lumsdon, A.E.; Berlekamp, J.; Tydecks, L.; Tockner, K. A global boom in hydropower dam construction. *Aquat. Sci.* **2015**, *77*, 161–170. [CrossRef]
3. St. Louis, V.L.; Kelly, C.A.; Duchemin, R.I.C.; Rudd, J.W.M.; Rosenberg, D.M. Reservoir surfaces as sources of greenhouse gases to the atmosphere: A global estimate. *Bioscience* **2000**, *50*, 766–775.
4. Deemer, B.R.; Harrison, J.A.; Li, S.; Beaulieu, J.J.; Delsontro, T.; Barros, N.; Bezerraneto, J.F.; Powers, S.M.; Santos, M.A.D.; Vonk, J.A. Greenhouse gas emissions from reservoir water surfaces: A new global synthesis. *Boioscience* **2016**, *66*, 949–964. [CrossRef]
5. Li, S.; Zhang, Q. Carbon emission from global hydroelectric reservoirs revisited. *Environ. Sci.Pollut. Res.* **2014**, *21*, 13636–13641. [CrossRef] [PubMed]
6. López Bellido, J.; Tulonen, T.; Kankaala, P.; Ojala, A. CO_2 and CH_4 fluxes during spring and autumn mixing periods in a boreal lake (Pääjärvi, southern Finland). *J. Geophys. Res. Biogeosci.* **2009**, *114*. G04007. [CrossRef]
7. Liu, H.; Zhang, Q.; Katul, G.G.; Cole, J.J.; Iii, F.S.C.; Macintyre, S. Large CO_2 effluxes at night and during synoptic weather events significantly contribute to CO_2 emissions from a reservoir. *Environ. Res. Lett.* **2016**, *11*, 064001. [CrossRef]
8. Roland, F.; Vidal, L.O.; Pacheco, F.S.; Barros, N.O.; Assireu, A.; Ometto, J.; Cimbleris, A.C.P.; Cole, J.J. Variability of carbon dioxide flux from tropical (Cerrado) hydroelectric reservoirs. *Aquat. Sci.* **2010**, *72*, 283–293. [CrossRef]
9. Gebremichael, A.W.; Osborne, B.; Orr, P. Flooding-related increases in CO_2 and N_2O emissions from a temperate coastal grassland ecosystem. *Biogeosciences* **2017**, *14*, 2611–2626. [CrossRef]
10. Harrison, J.A.; Deemer, B.R.; Birchfield, M.K.; O'Malley, M.T. Reservoir water-level drawdowns accelerate and amplify methane emission. *Environ. Sci. Technol.* **2017**, *51*, 1267. [CrossRef] [PubMed]
11. Oelbermann, M.; Schiff, S.L. Quantifying carbon dioxide and methane emissions and carbon dynamics from flooded boreal forest soil. *J. Environ. Qual.* **2008**, *37*, 2037–2047. [CrossRef] [PubMed]
12. Catalan, N.; von Schiller, D.; Marce, R.; Koschorreck, M.; Gomez-Gener, L.; Obrador, B. Carbon dioxide efflux during the flooding phase of temporary ponds. *Limnetica* **2014**, *33*, 349–359.
13. Dušek, J.; Čížková, H.; Czerný, R.; Taufarová, K.; Šmídová, M.; Janouš, D. Influence of summer flood on the net ecosystem exchange of CO_2 in a temperate sedge-grass marsh. *Agric. For. Meteorol.* **2009**, *149*, 1524–1530. [CrossRef]
14. Hu, Q.; Wu, Q.; Yao, B.; Xu, X. Ecosystem respiration and its components from a *Carex* meadow of Poyang Lake during the drawdown period. *Atmos. Environ.* **2015**, *100*, 124–132. [CrossRef]

15. Jin, H.; Yoon, T.K.; Lee, S.H.; Kang, H.; Im, J.; Park, J.H. Enhanced greenhouse gas emission from exposed sediments along a hydroelectric reservoir during an extreme drought event. *Environ. Res. Lett.* **2016**, *11*, 124003. [CrossRef]
16. Hou, C.; Song, C.; Li, Y.; Wang, J.; Song, Y.; Wang, X. Effects of water table changes on soil CO_2, CH_4 and N_2O fluxes during the growing season in freshwater marsh of northeast China. *Environ. Earth Sci.* **2012**, *69*, 1–9. [CrossRef]
17. Yang, M.; Geng, X.M.; Grace, J.; Jia, Y.F.; Liu, Y.Z.; Jiao, S.W.; Shi, L.L.; Lu, C.; Zhou, Y.; Lei, G.C. N_2O fluxes from the littoral zone of a Chinese reservoir. *Biogeosciences* **2015**, *12*, 4711–4723. [CrossRef]
18. Yang, M.; Geng, X.; Grace, J.; Lu, C.; Zhu, Y.; Zhou, Y.; Lei, G. Spatial and seasonal CH_4 flux in the littoral zone of Miyun Reservoir near Beijing: The effects of water level and its fluctuation. *PLoS ONE* **2014**, *9*, e94275. [CrossRef] [PubMed]
19. Gao, Z.Q. *Beijing Chronicles of Water Conservancy, Volume III*; Committee of the Beijing Chronicles of Water Conservancy: Beijing, China, 1989.
20. Cao, R.; Li, C.; Liu, L.; Wang, J.; Yan, G. Extracting Miyun Reservoirs water area and monitoring its change based on a revised normalized different water index. *Sci. Surv. Mapp.* **2008**, *33*, 158–160.
21. Burnham, K.P.; Anderson, D.R.; Huyvaert, K.P. AIC model selection and multimodel inference in behavioral ecology: Some background, observations, and comparisons. *Behav. Ecol. Sociobiol.* **2011**, *65*, 23–35. [CrossRef]
22. Zou, J.W.; Huang, Y.; Zheng, Z.H.; Wang, Y.S.; Chen, Y.Q. Static opaque chamber-based technique for determination of net exchange of CO_2 between terrestrial ecosystem and atmosphere. *Chin. Sci. Bull.* **2004**, *49*, 381–388. [CrossRef]
23. Kuzyakov, Y. Separating microbial respiration of exudates from root respiration in non-sterile soils: A comparison of four methods. *Soil. Biol. Biochem.* **2002**, *34*, 1621–1631. [CrossRef]
24. Stocker, T.F.; Qin, D.; Plattner, G.-K.; Tignor, M.; Allen, S.K.; Boschung, J.; Nauels, A.; Xia, Y.; Bex, V.; Midgley, P.M. *Climate Change 2013: The Physical Science Basis. Contribution of Working Group I to the Fifth Assessment Report of the Intergovernmental Panel on Climate Change*; Cambridge University Press: Cambridge, UK; New York, NY, USA, 2013.
25. Intergovernmental Panel on Climate Change (IPCC). *2006 Ipcc Guidelines for National Greenhouse Gas Inventories. Volume 4 Agriculture, Forestry and other Land Use*; Intergovernmental Panel on Climate Change: Bracknell, UK, 2006; Available online: http://www.Ipcc-nggip.Iges.Or.Jp/public/2006gl/index.htm (accessed on 17 September 2007).
26. Tranvik, L.J.; Downing, J.A.; Cotner, J.B.; Loiselle, S.A.; Striegl, R.G.; Ballatore, T.J.; Dillon, P.; Finlay, K.; Fortino, K.; Knoll, L.B.; et al. Lakes and reservoirs as regulators of carbon cycling and climate. *Limnol. Oceanogr.* **2009**, *54*, 2298–2314. [CrossRef]
27. Pace, M.L.; Prairie, Y.T. Respiration in lakes. In *Respiration in Aquatic Ecosystems*; Oxford University Press: New York, NY, USA, 2005; pp. 103–121.
28. Soumis, N.; Duchemin, E.; Canuel, R.; Lucotte, M. Greenhouse gas emissions from reservoirs of the western United States *Glob. Biogeochem. Cycles* **2004**, *18*. GB3022. [CrossRef]
29. Morales-Pineda, M.; Cózar, A.; Laiz, I.; Úbeda, B.; Gálvez, J.Á. Daily, biweekly, and seasonal temporal scales of pCO_2 variability in two stratified Mediterranean reservoirs. *J. Geophys. Res. Biogeosci.* **2014**, *119*. 2013JG002317. [CrossRef]
30. Jacinthe, P.A.; Filippelli, G.M.; Tedesco, L.P.; Raftis, R. Carbon storage and greenhouse gases emission from a fluvial reservoir in an agricultural landscape. *Catena* **2012**, *94*, 53–63. [CrossRef]
31. Demarty, M.; Bastien, J.; Tremblay, A.; Hesslein, R.H.; Gill, R. Greenhouse gas emissions from boreal reservoirs in Manitoba and Québec, Canada, measured with automated systems. *Environ. Sci. Technol.* **2009**, *43*, 8908–8915. [CrossRef] [PubMed]
32. Li, Z.; Zhang, Z.; Xiao, Y.; Guo, J.; Wu, S.; Liu, J. Spatio-temporal variations of carbon dioxide and its gross emission regulated by artificial operation in a typical hydropower reservoir in China. *Environ. Monit. Assess.* **2014**, *186*, 3023–3039. [CrossRef] [PubMed]
33. Metcalfe, D.B.; Fisher, R.A.; Wardle, D.A. Plant communities as drivers of soil respiration: Pathways,mechanisms, and significance for global change. *Biogeosciences* **2011**, *8*, 2047–2061. [CrossRef]
34. Lloyd, J.; Taylor, J. On the temperature dependence of soil respiration. *Funct. Ecol.* **1994**, 315–323. [CrossRef]
35. Xu, L.K.; Baldocchi, D.D.; Tang, J.W. How soil moisture, rain pulses, and growth alter the response of ecosystem respiration to temperature. *Glob. Biogeochem. Cycles* **2004**, *18*. GB4002. [CrossRef]

36. Banach, K.; Banach, A.M.; Lamers, L.P.; De Kroon, H.; Bennicelli, R.P.; Smits, A.J.; Visser, E.J. Differences in flooding tolerance between species from two wetland habitats with contrasting hydrology: Implications for vegetation development in future floodwater retention areas. *Ann. Bot.* **2009**, *103*, 341–351. [CrossRef] [PubMed]
37. Striker, G.G. Chapter 1—Flooding stress on plants: Anatomical, morphological and physiological responses. In *Botany*; Mworia, J., Ed.; InTech: Rijeka, Croatia, 2012; pp. 1–28.
38. Luo, Y.; Zhou, X. Chapter 5—Controlling factors. In *Soil Respiration and the Environment*; Luo, Y., Zhou, X., Eds.; Academic Press: Burlington, VT, USA, 2006; pp. 79–105.
39. McNicol, G.; Silver, W.L. Separate effects of flooding and anaerobiosis on soil greenhouse gas emissions and redox sensitive biogeochemistry. *J. Geophys. Res.Biogeosci.* **2014**, *119*, 557–566. [CrossRef]
40. Bolpagni, R.; Folegot, S.; Laini, A.; Bartoli, M. Role of ephemeral vegetation of emerging river bottoms in modulating CO_2 exchanges across a temperate large lowland river stretch. *Aquat. Sci.* **2017**, *79*, 149–158. [CrossRef]
41. Austin, A.T.; Ballaré, C.L. Dual role of lignin in plant litter decomposition in terrestrial ecosystems. *Proc. Nat. Acad. Sci. USA* **2010**, *107*, 4618–4622. [CrossRef] [PubMed]
42. Zenone, T.; Zona, D.; Gelfand, I.; Gielen, B.; Caminoserrano, M.; Ceulemans, R. CO_2 uptake is offset by CH_4 and N_2O emissions in a poplar short-rotation coppice. *Glob. Chang. Biol. Bioenergy* **2016**, *8*, 524–538. [CrossRef]
43. Merbold, L.; Eugster, W.; Stieger, J.; Zahniser, M.; Nelson, D.; Buchmann, N. Greenhouse gas budget (CO_2, CH_4 and N_2O) of intensively managed grassland following restoration. *Glob. Chang. Bioenergy* **2014**, *20*, 1913. [CrossRef] [PubMed]
44. Gao, B.; Xu, L.; Huang, W.; Ju, X.; Cui, S. Carbon benefits completely offset by nitrogen fertilization induced greenhouse gas emissions in Chinese main cropping systems. In Proceedings of the 2016 International Nitrogen Initiative Conference "Solutions to Improve Nitrogen Use Efficiency for the World"; Melbourne, Australia, 4–8 December 2016.
45. Tian, H.; Chen, G.; Lu, C.; Xu, X.; Hayes, D.J.; Wei, R.; Pan, S.; Huntzinger, D.N.; Wofsy, S.C. North American terrestrial CO_2 uptake largely offset by CH_4 and N_2O emissions: Toward a full accounting of the greenhouse gas budget. *Clim. Chang.* **2015**, *129*, 413–426. [CrossRef] [PubMed]
46. Audet, J.; Elsgaard, L.; Kjaergaard, C.; Larsen, S.E.; Hoffmann, C.C. Greenhouse gas emissions from a Danish riparian wetland before and after restoration. *Ecol. Eng.* **2013**, *57*, 170–182. [CrossRef]
47. Lee, S.C.; Christen, A.; Black, A.T.; Johnson, M.S.; Jassal, R.S.; Ketler, R.; Nesic, Z.; Merkens, M. Annual greenhouse gas budget for a bog ecosystem undergoing restoration by rewetting. *Biogeosciences* **2017**, *14*, 2799–2814. [CrossRef]
48. Järveoja, J.; Peichl, M.; Maddison, M.; Soosaar, K.; Vellak, K.; Karofeld, E.; Teemusk, A.; Mander, Ü. Impact of water table level on annual carbon and greenhouse gas balances of a restored peat extraction area. *Biogeosciences* **2015**, *13*, 2637–2651. [CrossRef]
49. Magnussen, S.; Reed, D. *Knowledge Reference for National Forest Assessments–Modeling for Estimation and Monitoring*; Food and Agriculture Organization of the United Nations: Rome, Italy, 2004.
50. Maqbool, C.; Khan, A.B. Biomass and carbon content of emergent macrophytes in Lake Manasbal, Kashmir: Implications for carbon capture and sequestration. *Int. J. Sci. Res. Pub.* **2013**, *3*, 1–7.
51. Tang, J.W.; Misson, L.; Gershenson, A.; Cheng, W.X.; Goldstein, A.H. Continuous measurements of soil respiration with and without roots in a ponderosa pine plantation in the Sierra Nevada Mountains. *Agric. For. Meteorol.* **2005**, *132*, 212–227. [CrossRef]
52. Hanson, P.J.; Edwards, N.T.; Garten, C.T.; Andrews, J.A. Separating root and soil microbial contributions to soil respiration: A review of methods and observations. *Biogeochemistry* **2000**, *48*, 115–146. [CrossRef]
53. Li, H.; Yang, M.; Lei, T.; Zhang, M.; Bridgewater, P.; Lu, C.; Geng, X.; Lei, G. Nitrous oxide emission from the littoral zones of the Miyun Reservoir near Beijing, China. *Hydrol. Res.* **2015**, *46*, 811–823. [CrossRef]